

Deciphering the groundwater–saline water interaction in a complex coastal aquifer in South India using statistical and hydrochemical mixing models

P. J. Sajil Kumar¹ 

Received: 23 October 2016 / Accepted: 31 October 2016 / Published online: 8 November 2016
© Springer International Publishing Switzerland 2016

Abstract Hydrogeochemical investigations were carried out in a coastal aquifer along the East coast of Cuddalore district in Tamil Nadu, Southern India, to analyse the groundwater–seawater interactions. Multiple techniques including Hydrochemical Facies Evaluation Diagram (HFE-D), principle component analysis (PCA), ionic ratios, hydrochemical ionic changes models and salinity mixing index (SMI) models were applied to refine the results and exactly understand the salinization process. EC and Ionic constituents along with the Gibbs plot showed controls of evaporation and the rock–water interaction on hydrogeochemistry, which is later proved by the bivariate plots. Major ions listed under PC1 (Na, Mg, Cl and SO₄) and PC2 (Ca, HCO₃, and CO₃) showing the influence of seawater and carbonate dissolution processes go together with cation exchange. Definitive results, shown by HFE-D plot than the piper plot, indicate that 58% of the samples either completely fall in the seawater zone or on the mixing line. Results of the ionic changes calculation indicate that 6 wells (50%) have a positive seawater fraction in the groundwater. Analogous results were observed for the SMI values (>1) in these wells, except in sample number 3. Encouragingly, after each method the results significantly rectified. Impact of seawater mixing with fresh groundwater is found in the entire stretch (perpendicular to coast) of samples in the southern end of the aquifer, and samples located in very near to the coast in the central part. Good

quality groundwater in the northern end indicate that the aquifer was unaffected by the seawater mixing.

Keywords Seawater–Groundwater mixing · HFE-D plot · Principle component analysis (PCA) · Hydrochemical ionic changes model · Salinity Mixing Index (SMI) model · Coastal aquifer · Tamil Nadu

Introduction

Deterioration of groundwater quality has strong correlation with population growth and industrialization. Most of the world's largest cities are located either near the rivers or the coasts. However, river water is insufficient to meet the ever-increasing demand of the cities. This scarcity of water has increased the overexploitation of groundwater. Groundwater serves as major and natural source of water for domestic and agricultural purposes in many cities (Mondal et al. 2010). However, groundwater quality in the coastal region is often under tremendous threat due to seawater intrusion (Somay and Gemici 2009; Melloul and Goldenberg 1997; Jørgensen et al. 2008; Cobaner et al. 2012; Werner et al. 2012). In the coastal regions, freshwater–saline water interface is highly mobile depending on the difference in hydraulic head. Overexploitation of freshwater through uncontrolled pumping is the normally encountered process that destroys the saline water–freshwater equilibrium. This naturally leads to salinization in the coastal regions (Pulido-Laboeuf 2004; Milnes and Renard 2004; Demirel 2004; Shammas and Jacks 2007; Kouzana et al. 2009). Salinization, consecutively, leads to an overall change in chemical composition of the groundwater (Richter and Kreitler 1993; Somay and Gemici 2009), especially proliferates the concentration of dissolved solids (TDS) and some chemical constituents such

✉ P. J. Sajil Kumar
pjsajil@gmail.com

¹ Hydrogeology Group, Institute of Geological Sciences, Freie Universität Berlin, Malteserstr. 74-100, 12249 Berlin, Germany

as Cl, Na, Mg, and SO₄ (Sukhija et al. 1996; Giménez and Morell 1997; Park et al. 2005).

The coastal aquifer systems are complex environments where geological heterogeneity, spatial and temporal variability in the flow field and surface water/groundwater interactions all play a crucial role in governing the distribution of fresh and saline waters (McInnis and Silliman 2010). Numerous studies were performed by researchers worldwide to identify and quantify seawater intrusion in coastal aquifers (Goldman et al. 1991; Yakirevich et al. 1998; Sivan et al. 2005; Prieto et al. 2006; Khublaryan et al. 2008). Multifarious methods are employed to study this widespread form of pollution, hydrogeochemical (Milnes and Renard 2004; Sarwade et al. 2007; Kouzana et al. 2009), Geophysical (Duque et al. 2008; de Franco et al. 2009; Zarroca et al. 2011), Isotope tracers (Jørgensen et al. 2008; Gattacceca et al. 2009; Han et al. 2011), numerical modeling (Abarca et al. 2007; Cobaner et al. 2012) and statistical analysis (Giménez and Morell 1997; Kim et al. 2005; Mondal et al. 2010).

The specific case of saline water–groundwater interaction was studied by Mondal et al. (2010) in a coastal watershed in South India using major ion chemistry. They have reported that freshwater with seawater mixed with a seasonal variability from 4.82 to 7.86% throughout the watershed. Another study by Kim et al. (2009) at Jeju Island, South Korea emphasized the usefulness of time-series data of EC and temperature at various depths for better understanding of the interaction processes between fresh and saline water. Sarwade et al. (2007) studied the seawater–groundwater mixing in a coral island system. Saline intrusion was identified as the main reason for the severe deterioration in groundwater quality.

The objective of the present study, carried out in a coastal aquifer located in the East Coast of South India, was to understand the groundwater–saline water mixing process. Multiple approaches including hydrochemical analysis, HFE-D plot, statistical techniques, hydrochemical Ionic changes and Salinity Mixing Index (SMI) were employed in the current study to ensure the accurate interpretation of the results.

Description of the study area

The study area is located in the East Coast of Tamil Nadu constituting the coastal regions of Cuddalore and Chidambaram Taluks. Geographically, this area lies between east longitude 79°22'00"–79°52'00" and north latitude 11°10'00"–12°50'00" (Fig. 1). Climate of this region is hot tropical with temperature ranging from 25 °C (December) to 31 °C (April). The summer season (March–May) is very humid. The annual normal rainfall for the period

(1901–2000) ranges from 1050 to 1400 mm. The South West monsoon follows till September and North East monsoon extents from October to December (CGWB 2009). The major rivers that drain the study area are Gadilam and Pennaiyar rivers in the North, Vellar and Coleroon in the South. They generally flow from West towards East and the pattern is mainly sub-parallel. All these rivers are ephemeral and carry floods during monsoon. Vellar, is another seasonal river, which drains the major portion in the southern part of the district. Manimuktha, Gomukhi and Mayura form the major tributaries which join the Vellar River (CGWB 2009).

A major portion of the study area is covered by eastern coastal plain, which is predominantly occupied by the flood plain of fluvial origin formed under the influence of Penniyar, Vellar and Coleroon river systems. Marine sedimentary plain is noted all along the eastern coastal region. In between the marine sedimentary plain and fluvial flood plains, fluvio-marine deposits are noted, which consist of sand dunes and back swamp areas. Black soils are observed in parts of Chidambaram Taluk. The younger alluvial soils are found as small patches along the stream and river courses in the district. Red sandy soil is seen covering the Cuddalore sandstone, laterite and lateritic gravels occurring in parts of Cuddalore Taluk (CGWB 2009). As the study area is typically a coastal region, the quaternary formations in the area consist of sediments of fluvial fluvio-marine and marine facies. It includes various types of soil, fine to coarse-grained sands, silts, clays laterite and lateritic gravels the semi consolidated formations are essentially argillaceous, comprising silts, clay stones, calcareous sandstones, siliceous limestones and algal limestones.

Materials and methods

Groundwater sampling and analytical techniques

Forty-nine groundwater samples were collected from the study area during January 2010. Each sample was located using a handheld GPS (HC Gramin). Wells were pumped out till the in situ parameters were stabilized. On-field measurements were conducted to determine the parameter such as electrical conductivity (EC) and pH. Alkalinity was measured by titration with 0.02 N H₂SO₄ prior to the groundwater sampling. Groundwater was collected in polyethylene bottles (1 L capacity); bottles were sealed and brought to the laboratory for analysis and stored properly (4 °C) before analysis. Analysis was carried out as per the standard methods suggested by APHA (1998). Major ions like Ca, Mg, Na, K, Cl, SO₄, NO₃ and F were analysed. Ca and Mg were analysed using titration with EDTA. Cl

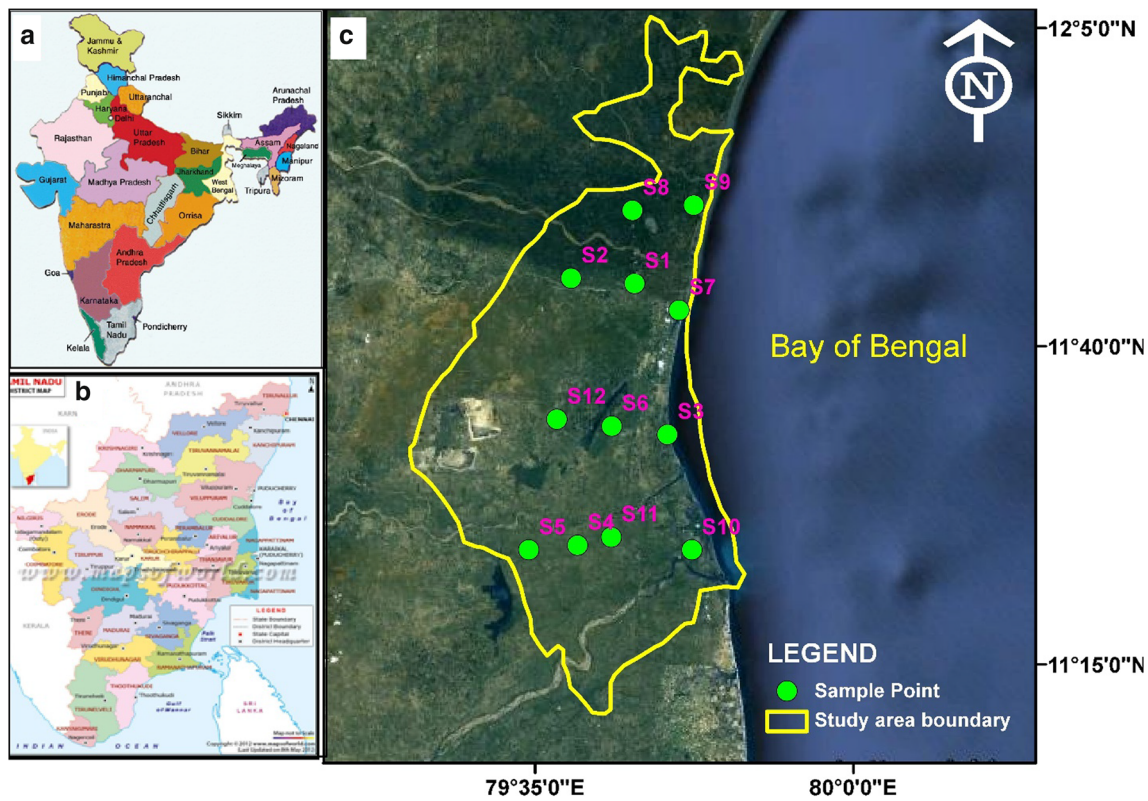


Fig. 1 The study area map showing **a** India. **b** Tamil Nadu. **c** Google earth Image of the study area and sampling points

concentration was determined using Argemetric titration. UV visible spectrophotometer was used for analysis of sulphate. Sodium and potassium were analysed using flame photometer. The analytical precision of the measurements of cations and anions is indicated by the ionic balance error, which has been computed on the basis of ions expressed in milliequivalent per liter (meq/L). The values were observed to be within the standard limit of $\pm 5\%$.

Hydrochemical facies evaluation

Conventional Piper plot (Piper 1953) and the more complicated HFE-D plot (Gimenez Forcada 2010) were employed to analyse the hydrochemical facies changes during the saline water–freshwater mixing in the study area. The HFE-D plot has 16 subdivisions, representing the various processes 1: Na–HCO₃/SO₄, 2: Na–MixHCO₃/MixSO₄, 3: Na–MixCl, 4: Na–Cl, 5: MixNa–HCO₃/SO₄, 6: MixNa–MixHCO₃/MixSO₄, 7: MixNa–MixCl, 8: MixNa–Cl, 9: MixCa–HCO₃/SO₄, 10: MixCa–MixHCO₃/MixSO₄, 11: MixCa–MixCl, 12: MixCa–Cl, 13: Ca–HCO₃/SO₄, 14: Ca–MixHCO₃/MixSO₄, 15: Ca–MixCl, 16: Ca–Cl. HFE-D can represent the main processes occurring during the intrusion and freshening stages in the evolution of the hydrochemical facies (Gimenez Forcada 2010; Ghiglieri

et al. 2012), which is not possible in the usual triangular plots including Piper trilinear diagram.

Principal component analysis (PCA)

Principal component analysis quantifies the relationship between the variables by computing the matrix of correlations for the entire data set. This helps to summarize the data set without losing much information (Rao et al. 2006). In the initial step, data sets were standardized and correlation matrix created. The eigenvalues and factor loadings for the correlation matrix were determined and scree plot was drawn. The extraction factors were based on the variances and co-variances of the variables. The eigenvalues and eigenvectors are evaluated, which represent the amount of variance explained by each factor. Eigenvalue greater than 1 was set as a criterion to extract factors (Kaiser 1958; Liu et al. 2003). Finally, by the process of rotation, the loading of each variable on one of the extracted factors is maximized and the loadings of all the other factors are minimized. These factor loadings are useful in grouping the water quality parameters and providing information for interpreting the data. This study considered pH, EC, Na, K Ca, Mg, Cl, CO₃, HCO₃ and SO₄ as water quality parameters. SPSS 16 was used for the Statistical analysis.

Hydrochemical ionic changes

Freshwater–seawater displacement can be evaluated depending on the calculation of the expected composition based on conservative mixing of seawater and freshwater in comparison to the result with actual compositions found in the studied groundwater samples (Appelo and Postma 2005). The seawater contribution was used to calculate the concentration of each ion (*i*) in the conservative mixing of seawater and freshwater (Eq. 1)

$$e_{i(mix)} = f_{sea} \times e_{i(sea)} + (1 - f_{sea}) \times e_{i(fresh)} \tag{1}$$

where e_i (in meq/L) is the concentration of specific ion (*i*), f_{sea} is the fraction of seawater in mixed freshwater–seawater, and subscripts mix, sea and fresh indicate the conservative mixture of seawater and freshwater. Any change in concentration (ionic change; $e_{i(change)}$), as a result of chemical reaction, can be expressed as shown in Eq. 2 (Fidelibus et al. 1993; Pulido-Laboeuf 2004).

$$e_{i(Change)} = [e_{i(sample)} - e_{i(mix)}] = [e_{i(sample)} - f_{sea} \times e_{i(sea)} + (1 - f_{sea}) \times e_{i(fresh)}], \tag{2}$$

where $e_{i(sample)}$ is the actual observed concentration of specific ion in the water sample. The fraction of seawater is normally based on Cl, which is a conservative ion with high solubility (Appelo and Postma 2005). The theoretical seawater fraction was calculated by considering the seawater contribution from the sample Cl concentration ($e_{Cl(sample)}$), the freshwater Cl concentration ($e_{Cl(fresh)}$) and seawater Cl concentration ($e_{Cl(sea)}$) (see Eq. 3) where, Cl concentration is expressed in milliequivalents per liter (meq/L) (Appelo and Postma 2005).

$$f_{sea} = [(e_{Cl(sample)} - e_{Cl(fresh)}) / (e_{Cl(sea)} - e_{Cl(fresh)})] \tag{3}$$

Seawater Mixing Index (SMI)

Seawater Mixing Index (SMI) is first suggested by Park et al. (2005). This parameter is based on the concentration of four major ionic constituents in seawater such as Na, Cl, Mg, and SO₄. It can be calculated using Eq. 4

$$SMI = a \times \frac{C_{Na}}{T_{Na}} + b \times \frac{C_{Mg}}{T_{Mg}} + c \times \frac{C_{Cl}}{T_{Cl}} + d \times \frac{C_{SO_4}}{T_{SO_4}} \tag{4}$$

where the constants a, b, c and d denote the relative concentration proportion of Na, Mg, Cl and SO₄ in seawater. C is the measured concentration in mg/L; and T represents the regional threshold values of the considered ions which can be estimated from the interpretation of cumulative probability curves.

Results and discussion

Hydrogeochemistry and its controlling mechanisms

The composition of the groundwater in the study area is presented in Table 1. Water quality of the region has varied considerably with range in TDS from 382 to 6032 mg/L. Among the 12 samples, 67% ($n = 8$) has crossed the guideline value for drinking 100 mg/L (WHO, 2011). All the groundwater samples were alkaline in nature (pH 8.00–9.00). Electrical conductivity, as a direct measure of salinity, showed significantly high values (up to 9630) in some of the wells adjoining the coast. These samples have undoubtedly affected by the seawater intrusion. In the major ion chemistry, Na, Mg, Cl and SO₄, in those wells located near the sea, were higher in concentration than the guideline values (WHO 2011). As expected for a coastal area, when the concentration of Ca becomes lower than the Na concentration, it represents the

Table 1 Results of the hydrogeochemical parameters of individual samples with respective geographical coordinates

S. no	Long.	Lat.	pH	EC	TDS	Ca	Mg	Na	K	Cl	SO ₄	CO ₃	HCO ₃
S1	79.71	11.75	8.7	630	382	32	12	101	5	50	5	36	256
S2	79.63	11.76	7.8	1110	721	56	36	156	4	160	111	0	342
S3	79.76	11.55	8.6	1270	813	26	22	205	73	230	80	30	268
S4	79.64	11.41	9	3470	2475	40	54	541	383	411	518	162	714
S5	79.58	11.40	8.6	3770	2700	48	88	823	3	610	701	72	683
S6	79.68	11.56	8.7	1180	692	34	22	196	5	110	154	42	250
S7	79.77	11.71	8.9	9690	6032	140	23	2001	125	2304	1056	114	476
S8	79.71	11.84	8.7	910	577	50	23	133	3	99	103	60	195
S9	79.79	11.85	8.4	760	484	32	26	129	4	71	72	24	244
S10	79.79	11.40	8.0	7330	4283	20	207	1242	45	2021	547	0	366
S11	79.68	11.42	8.4	1650	991	52	56	223	19	376	120	12	195
S12	79.61	11.57	8.2	710	457	38	28	87	4	128	60	0	189

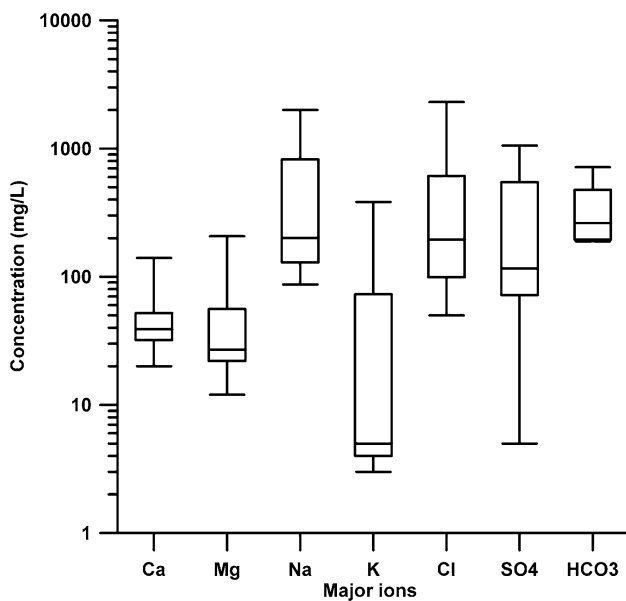


Fig. 2 Box plot displaying the distribution of statistical parameters in groundwater of the study area

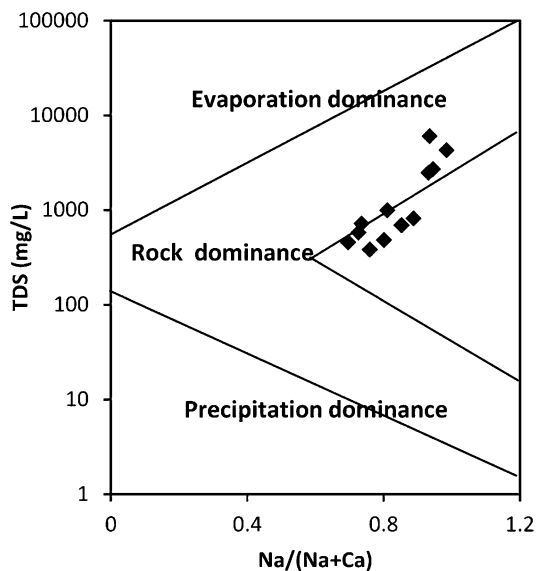


Fig. 3 Gibbs plot showing the mechanisms controlling the hydro-chemistry in the groundwater of the study area

natural discharge zone. The distribution of the statistical parameters of the groundwater in the study region is presented in Fig. 2. A Gibbs plot (Gibbs 1970) was drawn to identify the dominant mechanism controlling the hydrochemistry in the aquifer. As seen in Fig. 3, samples were plotted mainly in the rock dominant and evaporation dominant region in the plot. This shows the control of the aquifer lithology (rock dominance) and seawater mixing

(evaporation dominance) on groundwater chemical composition.

Evaluation of hydrochemical facies using Piper plot and HFE-diagram

The geochemical evolution of groundwater can be understood by plotting the concentrations of major cations and anions in the Piper trilinear diagram (Chidambaram et al. 2011). Hydrogeochemical facies in the groundwater of the study area is shown in a Piper plot (Fig. 4). Among the water types, 75% of the wells represented Na–Cl type indicating the influence of seawater mixing with fresh groundwater. The remaining samples plotted in the Na–Ca–HCO₃ and Ca–Mg–Cl type field. However, a detailed recognition of facies evolution sequence during recharge and encroachment events was not possible with Piper diagram (Ghiglieri et al. 2012). This difficulty is successfully overcome by the Hydrochemical Facies Evaluation diagram HFE-D suggested by Gimenez Forcada (2010). Groundwater samples from this study, which have been plotted in HFE-D plot, are presented in Fig. 5. In this figure, seawater (4) and freshwater fields (13) are connected through a mixing line. Other fields represent mixing sequences of major facies Na–Cl and Ca–HCO₃. The missing line represents the simple mixing between fresh groundwater and seawater (Samples 10–11–12) in the study area. Samples 3 and 7 are plotted in the seawater dominant field, while 4 & 5 showed a Na–MixCl nature. Sample 1,3,6,8 and 9 showed an assorted origin of facies; possibly dominated by the Na–Ca cation exchange process. The complexity of the salinization and the related hydro-geochemical processes in the study area is evident from this analysis, which needs to be studied more accurately as done in the forth section.

Principal component analysis (PCA) of the hydrochemical data

Correlation coefficient hydrogeochemical parameters ($n = 10$) for the groundwater samples ($n = 12$) are presented in Table 2. Strong positive correlations were found; pH with K ($r = 0.52$) and ($r = 0.82$), EC with Ca ($r = 0.62$), Mg ($r = 0.52$), Na ($r = 0.99$), Cl ($r = 0.98$), SO₄ ($r = 0.92$) and HCO₃ ($r = 0.51$), Na with Cl ($r = 0.96$), SO₄ ($r = 0.95$) and HCO₃ ($r = 0.51$), K with CO₃ ($r = 0.81$) and HCO₃ ($r = 0.66$), SO₄ with Cl ($r = 0.84$), CO₃ ($r = 0.61$), and HCO₃ ($r = 0.74$), CO₃ with HCO₃ ($r = 0.74$) etc. The strong positive correlation was observed for the ions such as Na, Cl, Mg and SO₄ with EC showing the dominance of these ions in the hydro-geochemistry of this area. However, the strong positive

Fig. 4 Piper trilinear plot showing the groundwater types in the study area

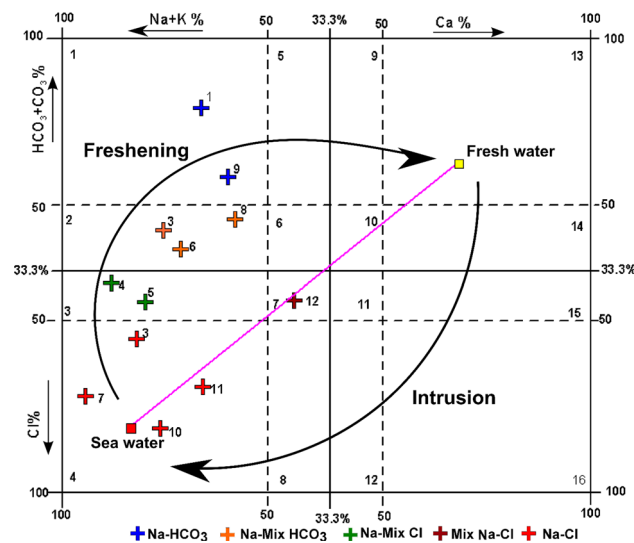
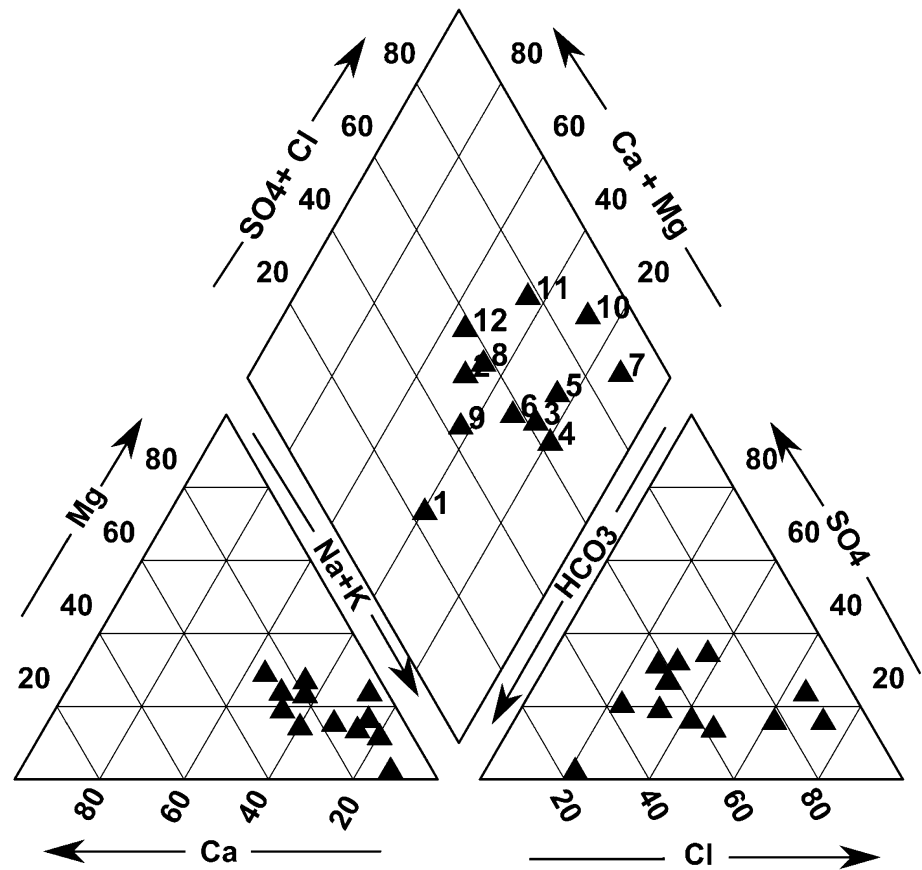


Fig. 5 Hydrochemical facies Evaluation diagram (HEF-D) explaining the seawater-groundwater mixing process

correlation of Ca with SO_4 is indicative of the dissolution of gypsum ion the aquifer.

Three principal components evolved as the hydrochemical parameters in the study area (see Fig. 6). The first component has higher factor loadings (>0.5) for ions such

as Na, Mg, Cl and SO_4 . These are the representative ions of seawater. The component 1 is responsible for 44% of the total variance in the dataset, indicating that these ions are dominating the groundwater chemistry. However, component 2 is responsible for 31% of the total variance in the analysed dataset. The dominant ions in this group are Ca, K, HCO_3 and CO_3 , demonstrating the dominance of rock-water interactions as well as the dissolution of carbonate minerals present in the aquifer. Mostly these ions have a terrestrial origin than marine dominance. This versatile result hints the mixing of waters from both terrestrial and marine origin. Component 3 showed strong negative correlation with Mg, HCO_3 and pH. These results have no definite trend that could be explained as a controlling factor of any of the process. However, this component can explain 16% of the total variance in the overall data.

Source evaluation of critical hydrochemical parameters

Ions like Na and Cl have a definite role in the evaluation of salinization process in the coastal regions (Wen et al. 2011; Shamma and Jacks 2007). Based on this common principle, the Na and Cl concentrations were drawn in a bivariate plot with a theoretical mixing line of freshwater and saline

Table 2 Correlation matrix for the hydrogeochemical parameters in the groundwater of the study area

	pH	EC	Ca	Mg	Na	K	Cl	SO ₄	CO ₃	HCO ₃
pH	1									
EC	0.15	1.00								
Ca	0.31	0.62	1.00							
Mg	-0.41	0.52	-0.26	1.00						
Na	0.20	0.99	0.68	0.43	1.00					
K	0.52	0.34	0.16	0.05	0.29	1.00				
Cl	0.02	0.98	0.56	0.57	0.96	0.21	1.00			
SO ₄	0.32	0.92	0.67	0.37	0.95	0.42	0.84	1.00		
CO ₃	0.82	0.40	0.44	-0.17	0.42	0.81	0.23	0.61	1.00	
HCO ₃	0.36	0.51	0.24	0.29	0.52	0.66	0.35	0.74	0.74	1.00

Bold values indicate significant correlation

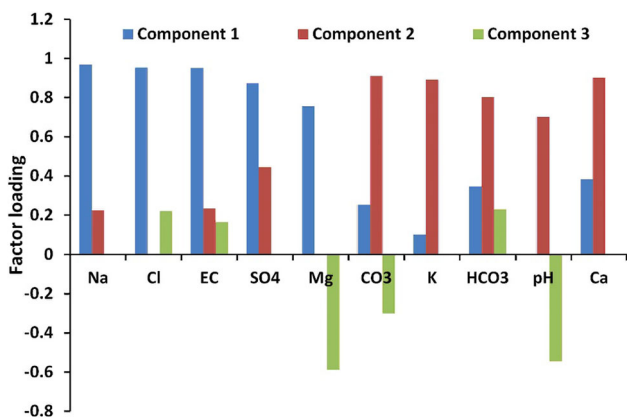


Fig. 6 Principle components of the hydrochemical parameters of the groundwater in the study area

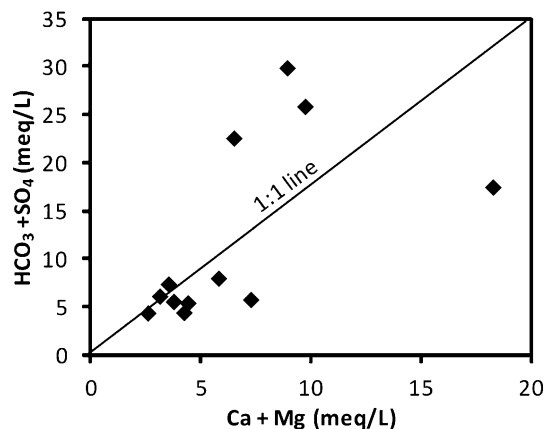


Fig. 8 Bivariate plot showing the relation between Ca + Mg and HCO₃ + SO₄, deciphering the control of carbonate dissolution and ion exchange process in the groundwater of the study area

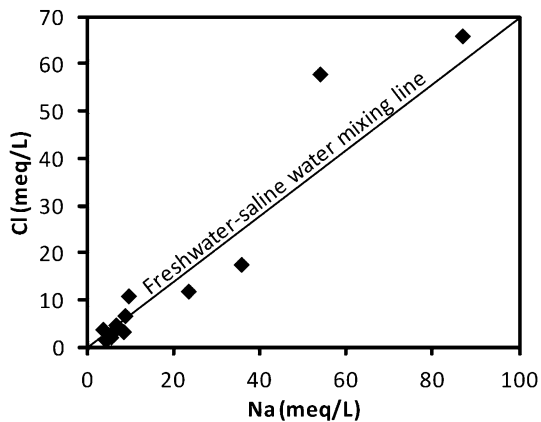


Fig. 7 Bivariate plot showing the relation between Na and Cl molar ratio. A theoretical mixing line is shown to differentiate the samples affected by seawater mixing and other processes in the groundwater of the study area

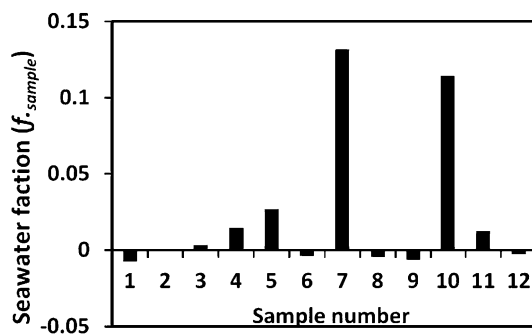
water (see Fig. 7). This analysis shows that many samples are plotted on or near the mixing line, indicating the influence of seawater mixing in the aquifer. Those samples

deviated from the general trend, which can be attributed to the other sources of Na or the cation exchange process modifying the groundwater chemistry by replacing it with Ca/and Mg.

The origin of Ca, Mg, HCO₃ and SO₄ will have a close relation if they are originated from dissolution of carbonate minerals (Wen et al. 2011). In their common origin, the groundwater samples will be plotted on or close to the Ca + Mg vs. HCO₃ diagram. In the study area, this plot shows a shift towards the lower upper part of 1:1 line (see Fig. 8). Those samples shifted down due to the excess of Ca + Mg compared to HCO₃, representing reverse ion exchange process. On the other hand, those samples shifted above the line due to the deficiency of Ca + Mg vs. HCO₃ + SO₄, indicating the normal ion exchange process. However, there are samples plotted on or near the 1:1 line showing the origin from dissolution of carbonate minerals. The positive correlations among these four minerals support the effect of carbonate minerals.

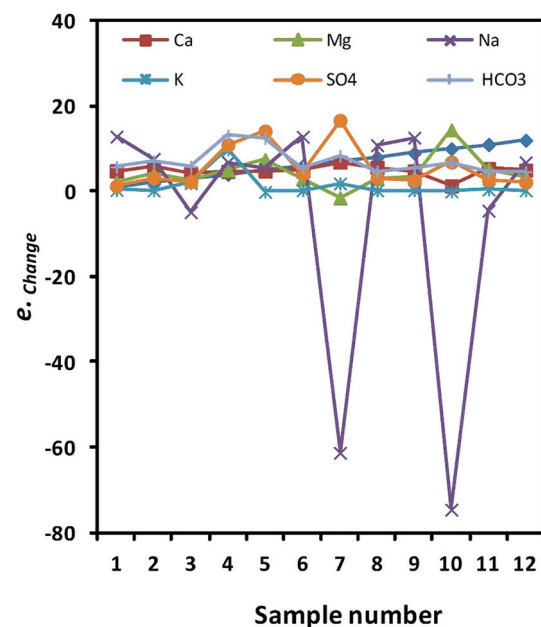
Table 3 Composition of seawater and freshwater (Appelo and Postma 2005) and fraction of seawater in individual samples

Ionic constituent	Seawater	Freshwater	S. no	Fraction of sample (f_{sample})
Ca	21.05	3.04	1	-0.007
Mg	32.3	0.99	2	-0.001
Na	1126	0.04	3	0.004
K	10.96	0.12	4	0.015
HCO ₃	1.49	5.83	5	0.027
Cl	461.11	4.48	6	-0.004
SO ₄	45.8	0.83	7	0.132
f_{sea}	100	0	8	-0.004
			9	-0.006
			10	0.114
			11	0.013
			12	-0.003

**Fig. 9** Plot showing the seawater fraction in individual samples. Positive values of f_{sample} indicate seawater mixing with fresh groundwater

Ionic changes during seawater–groundwater mixing

The results of the major ion chemistry, Piper diagram, principle component analysis and the Na vs. Cl cross plot indicate that hydrochemistry of the studied coastal aquifer is highly influenced by the seawater–groundwater mixing. The expected composition of the water during the freshwater–saline water displacement can be calculated based on the conservative mixing of seawater and freshwater. Later on, a comparison of the measured concentration with the actual seawater can effectively be used as a tool for describing the hydrochemical processes in the mixing zone (Aris et al. 2009). Using the Eqs. 1–3, based on the fact that Cl is a conservative tracer, seawater fraction in each sample was calculated (see Table 3; Fig. 9). Seawater fraction in each sample was utilized to calculate the ionic changes in Na, Ca, Mg, K, SO₄ and HCO₃ occurred during the interaction (Fig. 10). A positive seawater fraction (f_{sample}) was observed in 50% of the samples (S.nos: 3, 4, 5, 7, 10 and 11). Presence of seawater fraction in these samples is a clear indication of the mixing process. Since the Na content in the normal freshwater is less, Na_{change} will be positive in the fresh groundwater. In this study, the

**Fig. 10** Major ionic changes (e_{change}) in groundwater samples of the study area

sample numbers 3, 7, 10 and 11 showed negative values indicative of the contribution of seawater to the groundwater chemistry. This is in agreement with the result of f_{sample} , except sample numbers 4 and 5 as these samples are located slightly away from the coast. The most befitting explanation of this difference will be the cation exchange process which is already identified in “Principal component analysis (PCA) of the hydrochemical data”. However, being a conservative tracer, the Cl concentration remains unaltered with any external chemical reactions. It should be noted that the Ca_{change} was positive in all the samples including those which showed negative Na_{change} . The chemistry of the natural groundwater in the coastal area will be dominated by Ca and HCO₃ due to the carbonate

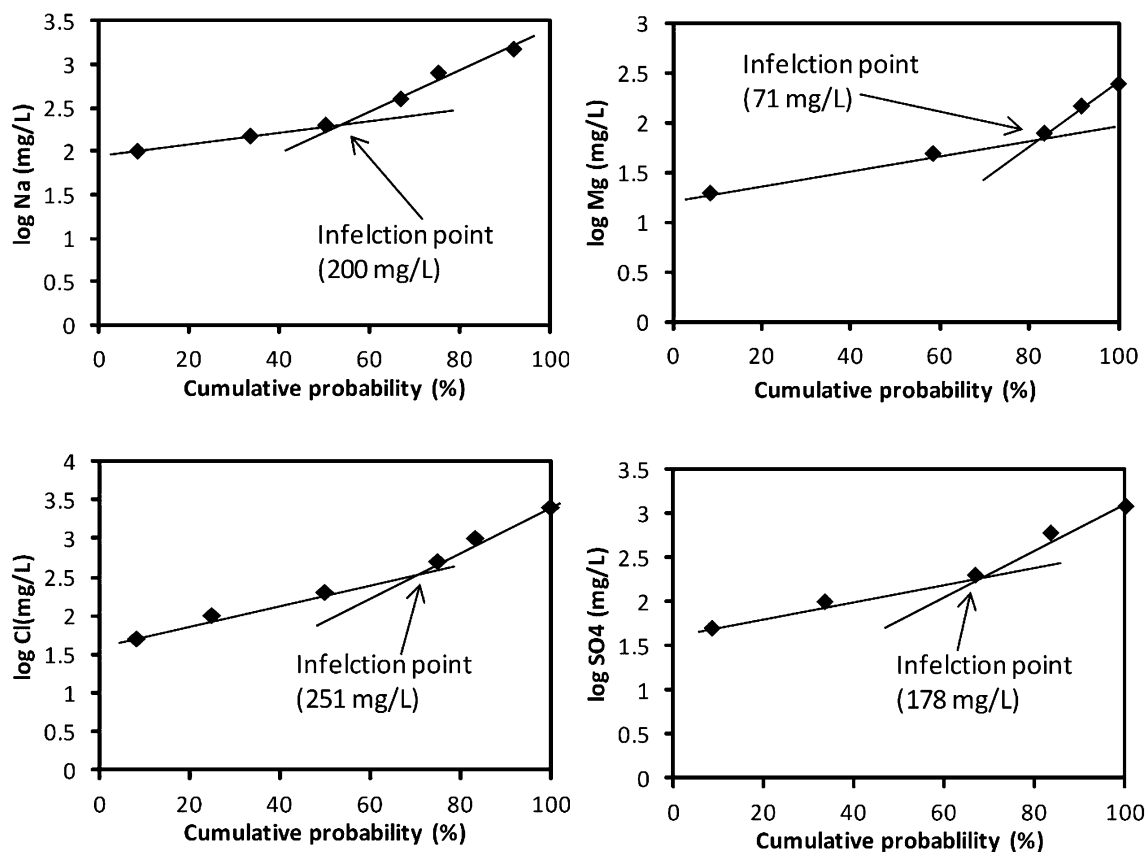


Fig. 11 Determination of the regional threshold values (T) of Na, Mg, Cl and SO₄ in the groundwater of the study area

dissolution (Mondal et al. 2011). In contrary to this, sea-water will be dominated by Na and Cl ions will be exchanged to the aquifer matrix during intrusion (Appelo and Postma 2005). However, this could be appropriately explained by the cation exchange in the costal aquifer, which is much more significant and better defined, and produces an inverse exchange between Na and Ca–Mg (Pulido-Laboeuf 2004). A negative K_{change} also supports the samples showed negative, Na_{change} and positive Ca_{change} . The declining trend in both Na and K, with increasing seawater fraction, indicates that the groundwater samples are dominated by seawater (Aris et al. 2009).

Evaluation of Seawater Mixing Index (SMI)

Seawater–groundwater mixing in the study area has been evaluated using the salinity mixing index (SMI). As input to the SMI equation expresses in Eq. 4, regional threshold values (T) of the critical parameters (Na, Mg, Cl and SO₄) have been calculated. Figure 11 illustrates the method of calculation of threshold values for the selected parameters. Cumulative probability percentages of the parameters were plotted against their logarithmic concentration value. The intersection point of each plot represents the T values of the

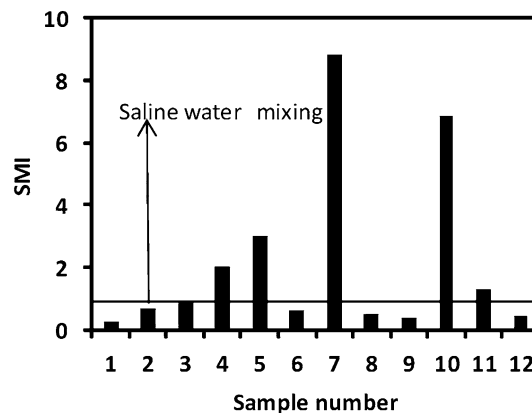


Fig. 12 Plot showing the Salinity Mixing Index (SMI) values in groundwater of the study area. SMII values greater than one indicating the influence of seawater mixing with fresh groundwater

corresponding ion (Sinclair 1974; Park et al. 2005). The determined T values of Na, Mg, Cl and SO₄ were 200, 71, 251 and 178 mg/L respectively. These T vales were substituted in Eq. 4 along with the relative concentration proportions ($a = 0.31, b = 0.04, c = 0.57, d = 0.08$) and the SMI values for each groundwater samples were deduced. If the calculated SMI value is greater than 1, the

water may be considered to unmistakably record the effect of seawater mixing (Park et al. 2005). The distribution of SMI in individual groundwater samples is presented in Fig. 12. Altogether, (4–5–7–10–11) 5 samples have showed an elevated SMI (>1), suggesting the impact of seawater mixing on the groundwater chemistry of the region. These results coincide with those of hydrochemical ionic change process, i.e. the same wells showed a positive seawater fraction (f_{sea}), except sample 3. This can be considered as further refinement in the result of ionic changes, supported by the lower salinity value (1270 $\mu\text{S}/\text{cm}$) as compared to the other high saline wells.

Conclusions

Groundwater chemistry in the coastal aquifer (part of Cuddalore and Chidambaram Taluks) shows that groundwater chemistry of the southern region, and to certain extent in the central region, is largely affected by the seawater mixing with the groundwater. The complexity of the hydrochemical processes in the study area is taken into account and a multidisciplinary approach was adopted for the accurate understanding. Though Piper diagram, a better delineation of the hydrochemical facies has been done using a complex HFE-D diagram. This plot was useful in differentiating the samples (nos: 3–4–5–7–10–11–12) affected by seawater mixing from the other processes like cation exchange. PCA analysis, demonstrates the positive correlation for EC with Ca ($r = 0.62$), Mg ($r = 0.52$), Na ($r = 0.99$), Cl ($r = 0.98$), SO_4 ($r = 0.92$) that illustrates 44% of the total variance of the total data set. This reveals that these variables are chiefly responsible for the groundwater chemistry of study area. However, the second component was useful in indicating more natural groundwater (Ca, K, HCO_3 and CO_3) with 31% of the total variability. Gibbs plot of the groundwater samples showed a definite trend for evaporation and rock water interaction dominance. This confirms the bivariate plots of Na vs. Cl and Ca + Mg vs. $\text{HCO}_3 + \text{SO}_4$ that salinization of the aquifer is a dominant process with active contribution from carbonate dissolution and cation exchange processes. Hydrochemical ionic changes and seawater mixing index (SMI) were applied particularly to demarcate the wells that have been influenced by the seawater–groundwater mixing. The seawater fraction in individual samples were calculated based on Cl (conservative tracer) concentration and identified that samples (3, 4, 5, 7, 10 & 11) had a positive seawater fraction. Moreover, the negative e_{change} for Na in these samples indicate the mixing of the seawater in these locations. Higher Salinity Mixing Index (SMI) values (>1) were observed for the same samples; except sample 3, that

showed slightly lower value than 1. However, this further confirms the dominance of seawater–groundwater mixing in the samples 4, 5, 7, 10 & 11.

All the methods used in this study proved instrumental in the exact demarcation of the seawater–freshwater mixing. A slight discrepancy was observed in the sample 12, which fell under the seawater–groundwater mixing line of HFE-Diagram and later left out from the seawater dominant wells grouped by Hydrochemical ionic changes and SMI. The location of this well (far away from the coast) and the permissible TDS value (457 mg/L) supported these argument. Another modification found is that sample 3 is excluded from the salinity affected wells reported by SMI, which was included in the ionic changes approach. It is clear that adopting manifold methods for a single problem will be helpful in comparing the results and obviously reducing the error in the assessment. This study concludes that all the wells located near the coast are affected by seawater intrusion except sample no. 12. Groundwater quality has deteriorated seriously in the southern end of the study area and to certain extent, in the central region. Overexploitation must be averted to protect the water quality and also to conserve a sustainable ecosystem.

References

- Abarca E, Carrera J, Sánchez-Vila X, Voss CI (2007) Quasi-horizontal circulation cells in 3D seawater intrusion. *J Hydrol* 339:118–129
- APHA (1998) Standard Methods for the Examination of Water and Waste Water, 20th edn. American Public Health Association, Washington DC
- Appelo CAJ, Postma D (2005) Geochemistry, groundwater and pollution, 2nd edn. Balkema, Rotterdam, pp 241–309
- Aris AZ, Abdullah MH, Ahmed A, Woong KK, Praveena SM (2009) Hydrochemical changes in a small tropical islands aquifer, Manukan Island, Sabah, Malaysia. *Environ Geol* 56:1721–1732
- CGWB (2009) District groundwater brochure Cuddalore district, Tamil Nadu. Technical report series
- Chidambaram S, Karmegam U, Prasanna MV, Sasidhar P, Vasanthavigar M (2011) A study on hydrochemical elucidation of coastal groundwater in and around Kalpakkam region, Southern India. *Environ Earth Sci* 64:1419–1431
- Cobaner M, Yurtal R, Dogan A, Motz LH (2012) Three dimensional simulation of seawater intrusion in coastal aquifers: a case study in the Goksu Deltaic Plain. *J Hydrol* 464–465(25):262–280
- de Franco R, Biella G, Tosi L, Teatini P, Lozej A, Chiozzotto B, Giada M, Rizzetto F, Claude C, Mayer A, Bassan V, Gasparetto-Stori G (2009) Monitoring the saltwater intrusion by time lapse electrical resistivity tomography: the Chioggia test site (Venice Lagoon, Italy). *J Appl Geophys* 69(3–4):117–130
- Demirel Z (2004) The history and evaluation of saltwater intrusion into a coastal aquifer in Mersin, Turkey. *J Environ Manag* 70(3):275–282
- Duque C, Calvache ML, Pedrera A, Martín-Rosales W, López-Chicano M (2008) Combined time domain electromagnetic soundings and gravimetry to determine marine intrusion in a detrital coastal aquifer (Southern Spain). *J Hydrol* 349(3–4):536–547

- Fidelibus MD, Gimenez E, Morell I, Tulipano L (1993) Salinization processes in the Castellon Plain aquifer (Spain). In: Custodio E, Galofre A (eds) Study and modelling of saltwater intrusion into aquifers. Centro Internacional de Metodos Numericos en Ingenieria, Barcelona, pp 267–283
- Gattacceca JC, Vallet-Coulomb C, Mayer A, Claude C, Radakovitch O, Conchett E, Hamelin B (2009) Isotopic and geochemical characterization of salinization in the shallow aquifers of a reclaimed subsiding zone: the southern Venice Lagoon coastland. *J Hydrol* 378(1–2):46–61
- Ghiglieri G, Carletti A, Pittalis D (2012) Analysis of salinization processes in the coastal carbonate aquifer of Porto Torres (NW Sardinia, Italy). *J Hydrol* 432–433:43–51
- Gibbs RJ (1970) Mechanisms controlling world water chemistry. *Science* 170:1088–1090
- Gimenez Forcada E (2010) Dynamic of sea water interface using hydro chemical facies evolution diagram. *Ground Water* 48(2):212–216
- Giménez E, Morell I (1997) Hydrogeochemical analysis of salinization processes in the coastal aquifer of Oropesa (Castellon, Spain). *Environ Geol* 29(1–2):118–131
- Goldman M, Gilad D, Ronen A, Melloul A (1991) Mapping of seawater intrusion into the coastal aquifer of Israel by the time domain electromagnetic method. *Geoexploration* 28(2):153–174
- Han D, Kohfahl C, Song X, Xiao G, Yang J (2011) Geochemical and isotopic evidence for palaeo-seawater intrusion into the south coast aquifer of Laizhou Bay, China. *Appl Geochem* 26(5):863–883
- Jørgensen NO, Andersen MS, Engesgaard P (2008) Investigation of a dynamic seawater intrusion event using strontium isotopes ($^{87}\text{Sr}/^{86}\text{Sr}$). *J Hydrol* 348(3–4):257–269
- Kaiser HF (1958) The varimax criteria for analytical rotation in factor analysis. *Psychometrika* 23(3):187–200
- Khublaryan M, Frolov A, Yushmanov I (2008) Seawater intrusion into coastal aquifers. *Water Resour* 35:274–286
- Kim Ji-Hoon, Kim Rak-Hyeon, Lee J, Cheong Tae-Jin, Yum Byoung-Woo, Chang Ho-Wan (2005) Multivariate statistical analysis to identify the major factors governing groundwater quality in the coastal area of Kimje, South Korea. *Hydrol Process* 19:1261–1276
- Kim KY, Park YS, Kim GP, Park KH (2009) Dynamic freshwater–saline water interaction in the coastal zone of Jeju Island, South Korea. *Hydrogeol J* 17:617–629
- Kouzana L, Mammou AB, Felfoul MS (2009) Seawater intrusion and associated processes: case of the Korba aquifer (Cap-Bon, Tunisia). *CR Geosci* 341(1):21–35
- Liu CW, Lin KH, Kuo YM (2003) Application of factor analysis in the assessment of groundwater quality in a blackfoot disease area in Taiwan. *Sci Total Environ* 313:77–89
- McInnis D, Silliman SE (2010) Geoelectrical investigation of the freshwater–saltwater interface in coastal Benin, West Africa, American Geophysical Union, Fall Meeting, abstract #H12B-04
- Melloul AJ, Goldenberg LC (1997) Monitoring of Seawater intrusion in coastal aquifers: basics and local concerns. *J Environ Manag* 51(1):73–86
- Milnes E, Renard P (2004) The problem of salt recycling and seawater intrusion in coastal irrigated plains: an example from the Kiti aquifer (Southern Cyprus). *Journal of Hydrology* 288(3–4, 30):327–343
- Mondal NC, Singh VP, Singh VS, Saxena VK (2010) Determining the interaction between groundwater and saline water through groundwater major ions chemistry. *J Hydrol* 388:100–111
- Mondal NC, Singh VS, Saxena VK, Singh VP (2011) Assessment of seawater impact using major hydrochemical ions: a case study from Sadras, Tamilnadu, India. *Environ Monit Assess* 177(1–4):315–335
- Park Seh-Chang, Yun Seong-Taek, Chae Gi-Tak, Yoo In-Sik, Shin Kwang-Sub, Heo Chul-Ho, Lee Sang-Kyu (2005) Regional hydrochemical study on salinization of coastal aquifers, western coastal area of South Korea. *J Hydrol* 313(3–4):182–194
- Piper AM (1953) A graphic procedure for the geo-chemical interpretation of water analysis. USGS Groundwater, Note no. 12
- Prieto C, Kotronarou A, Destouni G (2006) The influence of temporal hydrological randomness on seawater intrusion in coastal aquifers. *J Hydrol* 330(1–2):285–300
- Pulido-Laboeuf P (2004) Seawater intrusion and associated processes in a small coastal complex aquifer (Castrell de Ferro, Spain). *Appl Geochem* 19:1517–1527
- Rao NS, Devadas DJ, Rao KVS (2006) Interpretation of groundwater quality using principal component analysis from Anantapur district, Andhra Pradesh, India. *Environ Geosci* 13:239–259
- Richter BC, Kreitler WC (1993) Geochemical techniques for identifying sources of groundwater salinization. CRC Press, NY. ISBN 1-56670-000-0
- Sarwade D, Nandakumar M, Kesari M, Mondal N, Singh V, Singh B (2007) Evaluation of sea water ingress into an Indian atoll. *Environ Geol* 52:1475–1483
- Shammas M, Jacks G (2007) Seawater intrusion in the Salalah plain aquifer, Oman. *Environ Geol* 53:575–587
- Sinclair AJ (1974) Selection of thresholds in geochemical data using probability graphs. *J Geochem Explor* 3:129–149
- Sivan O, Yechieli Y, Herut B, Lazar B (2005) Geochemical evolution and timescale of seawater intrusion into the coastal aquifer of Israel. *Geochimica et Cosmochimica Acta* 69(3):579–592
- Somay MA, Gemici U (2009) Assessment of the salinization process at the coastal area with hydrogeochemical tools and Geographical Information Systems (GIS): Selçuk Plain, Izmir, Turkey. *Water Air Soil Pollut* 201:55–74
- Sukhija BS, Varm VN, Nagabhushanam P, Reddy DV (1996) Differentiation of paleomarine and modern seawater intruded salinities in coastal groundwaters (of Karaikal and Tanjavur, India) based on inorganic chemistry, organic biomarker fingerprints and radiocarbon dating. *J Hydrol* 174:173–201
- Wen X, Diao M, Wang D, Gao M (2011) Hydrochemical characteristics and salinization processes of groundwater in the shallow aquifer of Eastern Laizhou Bay, China. *Hydrol Process* 26(154):2322–2332
- Werner AD, Bakker M, Post VEA, Vandenbohede A, Lu C, Ataie-Ashtiani B, Simmons CT, Barry DA (2012) Seawater intrusion processes, investigation and management: recent advances and future challenges. *Adv Water Resour*. doi:10.1016/j.advwatres.2012.03.004
- WHO (2011) Guidelines for Drinking-water Quality, IV edn. World Health Organization, Geneva, p 340
- Yakirevich A, Melloul A, Sorek S, Shaath S, Borisov V (1998) Simulation of seawater intrusion into the Khan Yunis area of the Gaza Strip coastal aquifer. *Hydrogeol J* 6:549–559
- Zarroca M, Bach J, Linares R, Pellicer XM (2011) Electrical methods (VES and ERT) for identifying, mapping and monitoring different saline domains in a coastal plain region (Alt Empordà, Northern Spain). *J Hydrol* 409(1–2):407–422